Available online at www.sciencedirect.com

ScienceDirect

journal homepage: www.elsevier.com/locate/issn/15375110

Research Paper

Integration of visible branch sections and cherry clusters for detecting cherry tree branches in dense foliage canopies

*Suraj Amatya, Manoj Karkee**

Biological System Engineering, Center for Precision & Automated Agricultural Systems, Washington State University, WA, United States

ARTICLE INFO

Article history:
Received 30 October 2015
Received in revised form
3 May 2016
Accepted 21 June 2016
Published online 13 July 2016

Keywords:
Branch detection
Shake-and-catch cherry harvesting
Automated harvesting
Upright fruiting offshoots
Y-trellis canopy architecture

To minimise the demand for seasonal workers in sweet cherry production, there is a need to develop automated harvesting systems. The first step in automating a shake-and-catch type harvesting system is to develop a machine vision system for detecting tree branches and localising shaking points in those branches. In this study, an image processing algorithm was developed to detect branches of cherry trees using segmentation of branch and cherry pixels. Firstly, partially visible branch segments within the tree canopies were connected using morphological features of the segments to form whole branches. Then, the positions of cherry clusters in the canopy were used as an indication to detect branch sections that were occluded by cherries and leaves. Different cherry clusters were grouped together based on their spatial location and distance between them. Branch equations were then defined through those cherry clusters using minimum residual criteria. Overall, 93.8% branches were detected in a Y-trellis fruiting wall cherry orchard, with 55.0% of branches detected using only branch pixels and 38.8% additional branches detected using cherry clusters. The method resulted in a total of 12.4% of false positive detection. The results showed that branch detection accuracy can be substantially improved by integrating cherry location information with the location of segments of partially visible branches. This study has shown the potential of machine vision systems to detect cherry tree branches in full foliage season, which is highly promising for the development of automated sweet cherry harvesting systems.

1. Introduction

Sweet cherry harvesting is a highly labour intensive operation which constitutes more than 50% of total production costs (Seavert, Freeborn, & Long, 2008). Currently sweet cherry harvesting is carried out manually by semi-skilled seasonal labour. Thousands of cherries growing in random spatial locations on individual tree canopies make commercial hand-picking highly inefficient and costly (Li, Lee, & Hsu, 2011). With

* *Corresponding author*. Biological System Engineering, Center for Precision & Automated Agricultural Systems, Washington State University, 24106 N Bunn Rd, Prosser, WA 99350, United States. Tel.: +1 509 786 9208.
E-mail address: manoj.karkee@wsu.edu (M. Karkee).

http://dx.doi.org/10.1016/j.biosystemseng.2016.06.010
1537-5110/

Nomenclature

UFO	upright fruiting offshoots
USDA	United States Department of Agriculture
RDA	rapid displacement actuator
LED	light emitting diode
HFOV	horizontal field of view
x	feature vector
w_i	class definition
$P(w_i)$	prior probability of class w_i
$p(x\|w_i)$	class conditional distribution of x given that it belongs to class w_i
$p(w_i\|x)$	posterior probability of w_i given the evidence x
$p(x)$	probability of x
$di(x)$	decision function to decide class given the value of x
C_i	covariance matrix
m_i	mean vector
$\|C_i\|$	determinant of covariance matrix
Y	pixel position in rows
X	pixel position in columns
m	slope
C	intercept

the decreasing availability of agricultural workers and increasing labour costs, developing automated solutions for cherry harvesting has been one of the most critical needs of the sweet cherry industry around the world.

There are several factors that hinder the development of automated harvesting solutions including technological, economical and horticultural factors. Tree architecture is one of the important factors affecting the harvesting efficiency (Ampatzidis & Whiting, 2013). In recent years, growers of Washington State and other parts of the USA have been adopting more mechanisation-friendly plant architectures (Long, 2010; Peterson & Wolford, 2001). The upright fruiting offshoots (UFO) canopy architecture is one of the examples of a modern, planar training system that consists of trees with a permanent horizontal limb from which multiple vertical limbs are grown (Whiting, 2009). The UFO system may be trained to a vertical or Y-trellised architecture and provides a compact fruiting wall canopies. Investigations on mechanical harvesting have shown the potential to improve harvest efficiency by adopting the UFO training system (Chen et al., 2012; Du, Chen, Zhang, Scharf, & Whiting, 2011). This architecture is also amenable to automated harvesting aided by a machine vision system for fruit and branch detection.

Mechanisation of harvesting operation for various type of tree fruit and nuts has been widely investigated in the past with commercial success for various crops including nuts and fruit destined for processing market. One of the most widespread tree fruit harvesting techniques investigated and commercialised in the past is mechanical shaking (He et al., 2012), which has been investigated for several kinds of tree fruit crops including pistachio (Polat et al., 2006), apricot (Erdoğan, Güner, Dursun, & Gezer, 2003), olive (Blanco-Roldán, Gil-Ribes, Kouraba, & Castro-García, 2009), apple (Peterson, Bennedsen, Anger, & Wolford, 1999) and mango (Parameswarakumar & Gupta, 1991). A mechanical harvester developed and comprehensively evaluated by United States Department of Agriculture (USDA) in early 2000's (Peterson & Wolford, 2001) was based on engaging a rapid displacement actuator (RDA) on a limb using a manual controller. Evaluations of the efficiency of this prototype mechanical harvester revealed the difficulty for the operators to position the actuator due to the limited viewing angle from the operator's fixed seated position (Peterson, Whiting, & Wolford, 2003). A subsequent study of the harvester reported a significant effect of orchard characteristics and operator performance on the harvesting speed (Larbi & Karkee, 2014). In addition, multilayer catching surfaces located very close to the canopy may be essential to improve collection rate and reduce fruit damage rate during mechanical harvesting (observation based on ongoing work at Washington State University). However, this type of collection mechanism will critically limit the visibility and ability of an operator to localise branches for shaking. To address this issue, there is a need to develop an automated harvester using a machine-vision-based system for detecting branches, identifying shaking points and positioning the end-effector.

Various investigations have been conducted in the past to detect and reconstruct branches and trunks of fruit trees (Karkee & Adhikari, in press; Karkee, Adhikari, Amatya, & Zhang, 2014; Tabb, 2009; Wang & Zhang, 2013). However, most of these studies have focused on detecting branches in dormant season with potential application in pruning and crop-load management. Machine vision has also been widely investigated in the past for automating tree fruit harvesting operation. Some examples include the machine vision systems studied for harvesting apples (Baeten, Donne, Boedrij, Beckers, & Claesen, 2008), oranges (Slaughter & Harrell, 1989), peaches (Kurtulmus, Lee, & Vardar, 2014), and cherries (Amatya, Karkee, Gongal, Zhang, & Whiting, 2016; Tanigaki, Fujiura, Akase, & Imagawa, 2008). Tanigaki et al. (2008) developed a 3D machine vision system for picking cherries form tree canopies in greenhouse environment. Most of these studies are focused on identifying individual fruit for selective harvesting. However, only limited studies have been reported in investigating machine vision system for fruit harvesting using bulk harvesting techniques such as branch shaking.

Amatya et al. (2016) developed a method for detecting branches to automate cherry harvesting using branch shaking. They used partially visible branch sections in a full foliage canopy to reconstruct cherry tree branches and reported an accuracy of 89.2% in a vertical architecture with relatively lighter canopy density (Fig. 1a). With higher density of foliage and cherry clusters, the branch visibility may decrease drastically (Fig. 1b), limiting the accuracy of branch detection method using visible branch segments. However, as cherries grow along the branches, location of cherry clusters can be useful in estimating location of branches that are hidden by cherries and leaves. The specific objective of this study is to integrate the sections of partially visible branches and location of clusters of cherries to detect cherry tree branches in the presence of dense foliage during harvest season. The result can be used to guide the actuating mechanism of a harvester to tree branches for automated cherry harvesting.

Fig. 1 – a) Cherry tree branches trained in a vertical architecture with a light foliage density (Amatya et al., 2016); and b) Cherry tree branches in a Y-trellis system with higher foliage and fruit density.

2. Materials and methods

The branch detection method primarily included image acquisition in an experimental cherry block, followed by segmentation of branch and cherry pixels. Then, fully or partially visible branches were detected using segmented branch regions. In addition, segmented cherry clusters were used to detect occluded branches. The result of the branch detection method included branches detected using only branch pixels as well as the branches detected using cherry pixels. The performance of branch detection algorithm was assessed by comparing the final result with results from manual branch counting completed in the field for canopy regions captured by the field of view of camera. More details in these steps are provided in the following paragraphs.

2.1. *Image acquisition*

Image acquisition for this research was carried out in the WSU experimental orchard in Prosser, WA, USA. The cherry trees were trained to Y-trellis architecture with fruiting limbs oriented about 55° from the horizontal plane. The test orchard had a tree spacing of 4.3 m × 1.7 m and tree height of approximately 3.5 m. To avoid the variability in natural illumination, image acquisition was carried out during the night with controlled lighting conditions provided by LED lights (Trilliant® 36 Light Emitting Doide Grote, Madison, IN, USA). A stereo vision device (Bumblebee® XB3, Point Grey Research Inc., B.C., Canada) was used in this study to acquire images. Bumblebee camera included three lenses with maximum resolution of 1280 × 960 pixels, aligned horizontally at 12 cm spacing. Each lens had a focal length of 6 mm with 43° horizontal field of view (HFOV). A single image per tree, taken from the central lens was used for this study. The camera was mounted about 0.5 m above ground on a utility vehicle, Gator™ (Deere & Company, Moline, IL, USA) such that the camera is pointed vertically upwards (Fig. 2).

2.2. *Image classification*

A Bayesian classifier was used to classify image pixels into four classes, namely: branches, cherries, leaves and background. A Bayesian classifier is a pattern classification technique based on probability theory, which uses the knowledge of probability distribution to make classification decisions with least expected error rate (Shapiro & Stockman, 2001). This technique is based on Bayes rule, which estimates the posterior probability of classifying a pixel into a class based on the similarity of features as well as knowledge about the priori probability (prior) of occurrence of a particular class (Duda, Hart, & Stork, 1973). The input parameters for Bayesian classifier is a multivariate feature vector, x, for all classes w_i. The Bayesian classifier has the decision function of the form:

$$d_i(x) = \ln P(w_i) - \frac{1}{2}\ln|C_i| - \frac{1}{2}\left[(x - m_i)^T C_i^{-1}(x - m_i)\right] \quad (1)$$

where $P(w_i)$ is the prior probability, which is defined as the percentage of feature vectors belonging to a class w_i with respect to total number of feature vectors. C_i and m_i are the covariance matrix and mean of the feature vector of class w_i, and $|C_i|$ is the determinant of C_i (Gonzalez & Woods, 2002).

The Bayesian classifier was trained using 20 cherry tree images. Training images were manually segmented into branch, cherry, leaf and background classes. Red, green and blue intensity values were extracted for each class and used as the feature vector for training the classifier. Detailed explanation on image classification method used in this work can be found in Amatya et al. (2016), which has reported a classification accuracy of 91.0%, 73.0%, 90.9% and 91.2% respectively for branch, cherry, leaf and background classes. The mean and covariance of the feature vectors estimated by Amatya et al. (2016) were used as Bayesian classification parameters for image classification in this study. The pixel-level classification accuracy for cherry tree images used in this study was evaluated with a test data set of 50 randomly selected images.

2.3. *Branch detection using branch pixels*

A method developed by Amatya et al. (2016) for detecting tree branches using visible branch segments was applied to detect cherry tree branches. The detection method used the morphological features of visible branch segments including orientation, length and thickness to group branch segments together. Individual branch segments were identified as the

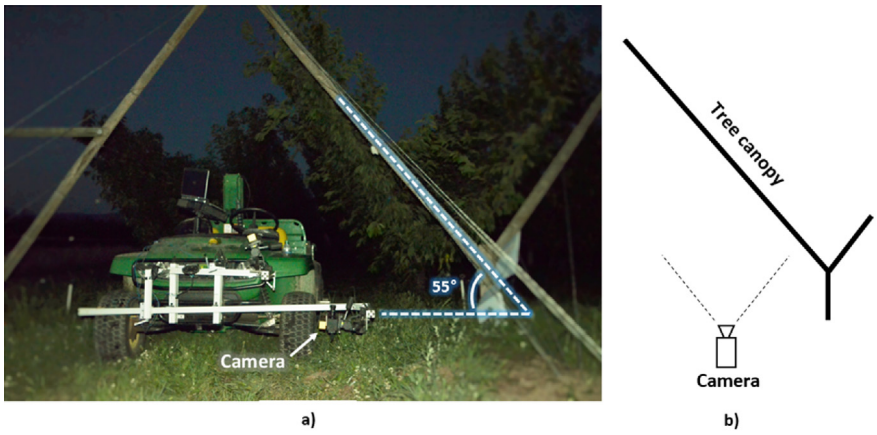

Fig. 2 – a) Sensing system used in the study to acquire images of cherry trees trained in Y-trellis architecture. Image acquisition was carried out in night time using LED lights (Trilliant® 36, Grote); b) schematic diagram showing camera position relative to tree canopy.

part of the same branch when two or more segments were oriented in same direction. Additionally, all branch segments longer than 80 mm were also detected as individual branches. Every branch detected by the algorithm was represented by an equation that approximated the medial axis of the branch. Linear model and logarithmic models (Eqs. (2) and (3)) were fitted to the branch pixels and the model with least residual value was selected as the best fitted branch equation. For detailed description of branch detection method using visible branch segments, please refer to Amatya et al. (2016).

$$\text{Linear Model}: \quad Y = mX + C \tag{2}$$

$$\text{Logarithmic Model}: \quad Y = m\log(X) + C \tag{3}$$

where Y is pixel position in rows, X is pixel position in columns, m is the slope of the line representing the branch and C is the model intercept.

2.4. *Combining branch and cherry regions for improved branch trajectory*

The previous method of branch detection could yield broken branches when the orientation of different visible sections of same branch differed by more than 20°, which in turn could lead to the detection of the same branch multiple times. Figure 4(b) shows an example of branch regions obtained after image segmentation of cherry tree images. By implementing the orientation and length-based branch detection method discussed in previous subsection, two branch sections oriented in different directions were detected as shown in Fig. 4(c). Integration of branch and cherry regions in the neighbourhood of previously detected branches was carried out to improve the accuracy of branch detection method. Starting from the longest detected branch section, the branch section was extended by approximately 150 mm (100 pixels) on either side along the corresponding branch trajectory defined by the model equation. The region within 30 mm (20 pixels) on the lateral direction of the branch trajectory was considered as the neighbourhood zone. If any branch or cherry region fell within the neighbourhood zone, those branch and cherry regions were included to be the parts of the same branch and the branch equation was updated. The branch was then extended along the new branch trajectory to identify if any other branch or cherry regions are in its neighbourhood. This process continued until no further addition took place. Figure 3(d) shows the end result of this branch merging method, which combined the previously unassigned branch regions to form a longer branch. In addition, cherry regions in the neighbourhood of branch trajectory (vertically striped; Fig. 4d) were also merged with detected branch region to form longer branch sections.

2.5. *Cherry pixel-based branch detection*

Detection of branches based on branch pixels was successful in canopy regions with low foliage density where branches were fully or partially visible. In the canopy regions with high foliage and fruit density, branches were heavily occluded (some even completely occluded), which led to a substantial proportion of undetected branches. In addition, branch visibility was critically low when the tree branches were small in diameter with dense foliage and cherry clusters around them. In such conditions, the method for detecting branches based on only branch pixels led to a low branch detection accuracy. Detection of cherry clusters provided useful information in detecting branches that are occluded by foliage or cherry clusters. Cherry clusters are located in a close proximity to the branch bearing them and completely occluded some branches. In a UFO cherry orchard used in this study, a number of cherry clusters aligned closely in a vertical direction indicated the presence of a branch along those clusters. When multiple cherry clusters were identified in such a fashion, a branch was assumed to be located at that position and a curve passing through those clusters was fitted.

Before using cherry clusters to detect occluded branches, cherry clusters associated with visible branches were removed to avoid multiple detection of previously detected branches. This was achieved by assigning all cherry regions near the detected branches as the part of the same branch and excluding such regions in the following steps of branch

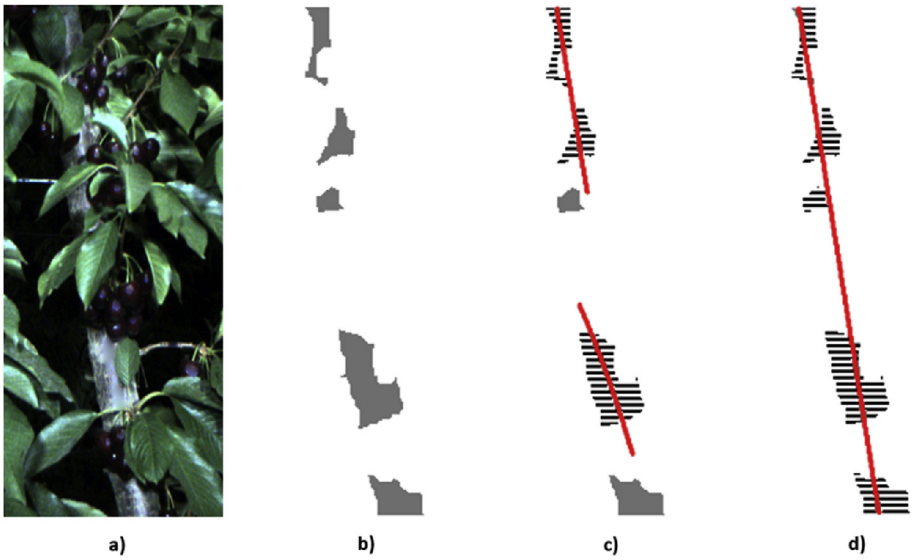

Fig. 3 – a) Original image; b) segmented branch regions (solid grey regions); c) branch detection; striped regions represented branch segments assigned to a branch; solid grey regions represent branch regions not detected as a part of any branches; d) improved branch trajectory representing the branch detected after integration of neighbourhood branch regions.

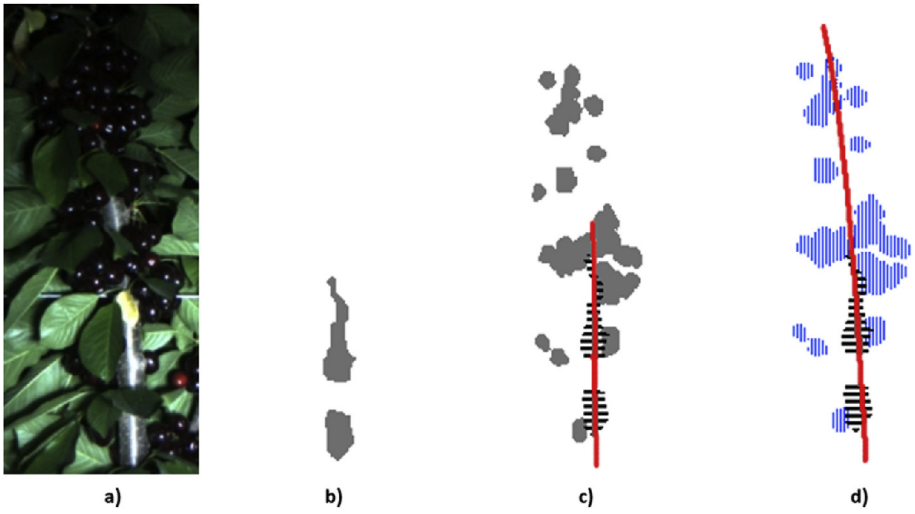

Fig. 4 – a) Original image; b) segmented branch region (solid grey regions); c) branch detection; horizontally striped regions represent detected branch segments; solid grey regions are segmented cherry regions; d) improved branch detection by combining cherry regions in the neighbourhood of previously detected branch trajectory.

detection. The segmented cherry pixels and the branch equations identified using branch sections were used as the inputs in this step of detecting branches with cherry pixel information. For each of the previously identified branches, a neighbourhood search region was defined along the branch section (as defined by the equation) with a specified lateral offset proportional to the width of the branch. The neighbourhood search method was similar to the one carried out for updating branch equations as described in previous subsection, except that a much larger lateral offset (minimum 50 pixels; approx. 80 mm) was used in this case. Any cherry region found in the neighbourhood was marked with the respective branch identifier but the branch equation was not updated this time. After all cherry clusters in the neighbourhood of detected branches were labelled, the remaining unmarked cherry regions were used in the next step for detecting new branches using only spatial location of cherry clusters. The major steps involved in detecting cherry tree branches using location of cherry clusters is shown in the flowchart below (Fig. 5) and described in the following paragraphs.

The remaining cherry regions, which were not associated with any previously detected branches, were used to predict new branches. Unlike branch segments, orientation of cherry clusters cannot be used as an indicator of branch orientation because the clusters are irregular in shape. Therefore, to detect branch orientation in this case, a region growing approach was used. Starting at the bottom of the image and

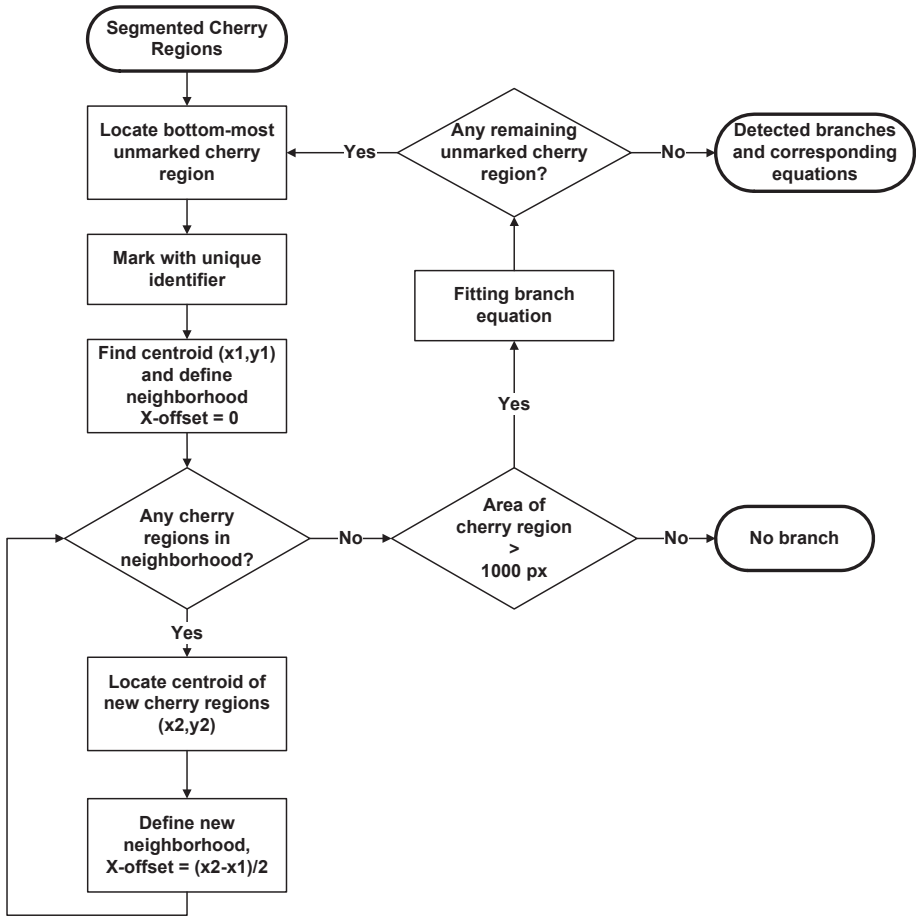

Fig. 5 – Flowchart showing major steps in branch detection using cherry pixel regions.

gradually moving upwards, cherry clusters potentially belonging to the same branch were identified. First, the bottom-most cherry region was located in the segmented image and was labelled with a unique identifier as a parent region. A neighbourhood was defined covering 200 pixels above and 15 pixels below the topmost point of the region and 75 pixels in the lateral direction around the centroid of the region (Fig. 6). These parameters were selected using trial and error method for the given tree architecture, camera resolution and imaging distance. If any other cherry region was found in that neighbourhood, those were labelled with the same label as the parent region and the centroid of newly added regions were located. Denoting the centroid of parent region as (x_1, y_1) and the centroid of new region/regions as (x_2, y_2), the total offset of centroid in x-axis was equal to $x_2 - x_1$. New neighbourhood search region was then defined above the new region with an offset value of $(x_2 - x_1)/2$ in the x-axis (Fig. 7). This centroid offset value was used to adjust the trajectory of search region according to the potential orientation of the branch to which these cherry clusters belong. This process of neighbourhood search was repeated until no new regions were found.

When no more cherry regions were found in the vertical direction, the next unassigned cherry region at the bottom of the region was located as a new parent region. Then the same

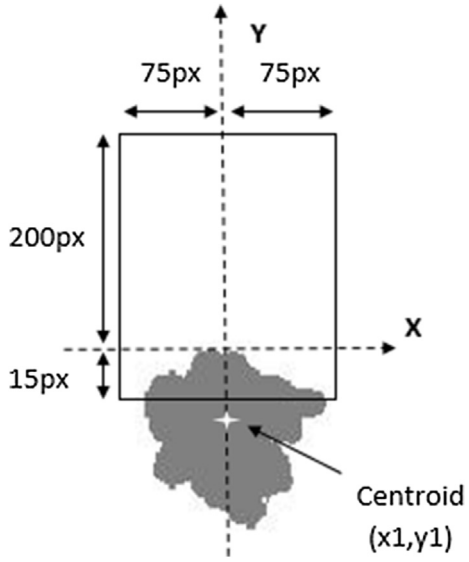

Fig. 6 – A neighbourhood for identifying cluster of cherries around a given cluster for predicting a branch passing through them.

process of neighbourhood search was repeated to add new cherry clusters to the new parent region. After all cherry regions were grouped with individual parent regions, the overall area of each group was estimated. If the cluster group had the

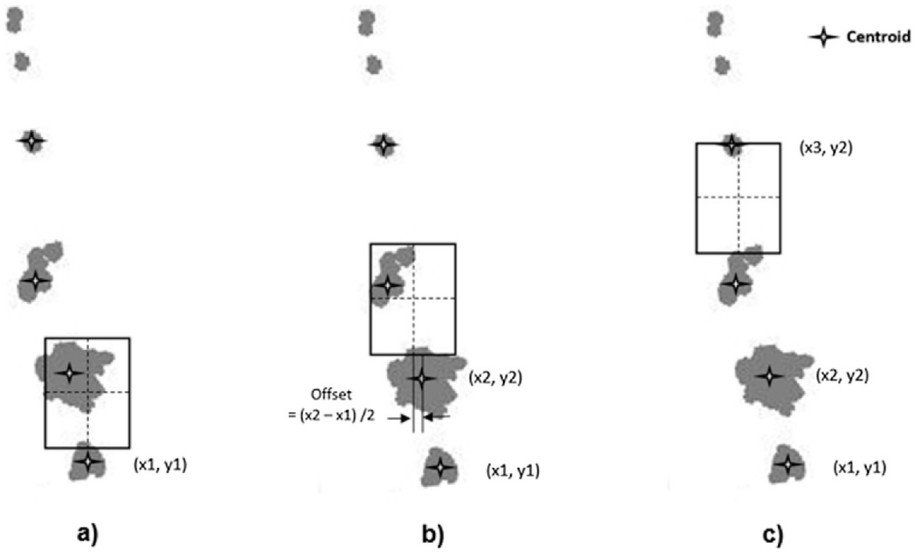

Fig. 7 – Progression of the region growing method with a neighbourhood search around a cherry region; a) first step from bottom-most region with no offset in *x*-axis; b) second step with an *x*-axis offset of $(x_2 - x_1)/2$; and c) third step with *x*-axis offset of $(x_3 - x_2)/2$.

pixel area less than 1000 pixels (roughly three cherries or less), those groups were rejected from the potential list of branches. For each remaining cherry groups, linear and logarithmic models were fitted. The equation with the lowest residual was then selected as the best to define each of those branches. Two sets of branch equations determined in this and previous sub-sections were then combined as the final result of the branch detection method.

3. Results and discussions

3.1. *Pixel classification*

Image pixels were classified as one of the four classes: branches, cherries, leaves or background. The mean and covariance of feature vector for each class that were used for image classification (Amatya et al., 2016) are shown in Table 1. Performance of the classification method was evaluated with a data set of 50 test images (Table 2). Consumers' accuracy, which is defined as the fraction of correctly classified pixels with respect to all pixels classified as that class, for branch and cherry pixel were found to be 81.4% and 95.5% respectively. Relatively lower consumers' accuracy was achieved for the branch class because of misclassified pixels to this class from cherry and leaf classes. Cherry pixels, on the other hand, were classified with high consumers' accuracy. However, producers' accuracy, which is defined as the fraction of correctly classified pixels with respect to all the pixels belonging to that class, was estimated to be only 60.0% for cherry pixels. It was also observed that about 35.2% of cherry pixels were misclassified as background. The main reason was the dark colour of cherries, which was similar to the background colour. Mostly the cherry pixels from the areas with low illumination were classified as being from the background. For the application in branch detection, it was desirable to have higher consumers' accuracy to ensure that smaller percentage of misclassified pixels are present in a segmented region, which can be removed using morphological operations and other noise filtering techniques.

Table 1 – Mean feature vector for branch, cherry, leaf and background classes.

	Red (R)	Green (G)	Blue (B)
Branch	128	145	155
Cherry	39	304	38
Leaf	76	130	94
Background	12	21	15

3.2. *Tree branch detection*

A total of 138 images were evaluated for this study containing a total of 453 cherry tree branches. An example of overall branch detection process is shown in Fig. 8. Figure 8(a) shows an original image of the cherry tree, Fig. 8(b) shows branches detected using only branch pixels, and Fig. 8(c) shows branches detected using both branch and cherry pixels. The lines with square markers in the figure represent branches identified using branch pixels whereas the lines with circular markers represent branches identified using cherry pixels.

It was found that 55.0% of branches were identified using only the branch pixels (Table 3). The detection accuracy with only branch pixel information was low because a substantial number of branches were occluded by the foliage and cherry clusters. When cherry regions were used to help predict occluded branches, additional 38.8% of previously invisible branches were detected, leading to the total branch detection accuracy of 93.8%. The rate of false positives in branch detection was 4.6% and 7.7% while using branch pixels and cherry pixels respectively. False positives were defined when there was no actual branch existed in the image or when the actual location and/or orientation of the branch were different than the predicted.

Table 2 – Confusion matrix depicting the performance of pixel classification method.

		Actual (pixels)				Consumers' accuracy
		Branch	Cherry	Leaves	Background	
Predicted	Branch	39,953	3498	5060	597	81.4%
	Cherry	1189	48,066	135	928	95.5%
	Leaves	2563	355	445,715	22,263	94.7%
	Background	1070	28,177	22,696	443,893	89.5%
Producers' accuracy		89.2%	60.0%	94.9%	94.9%	

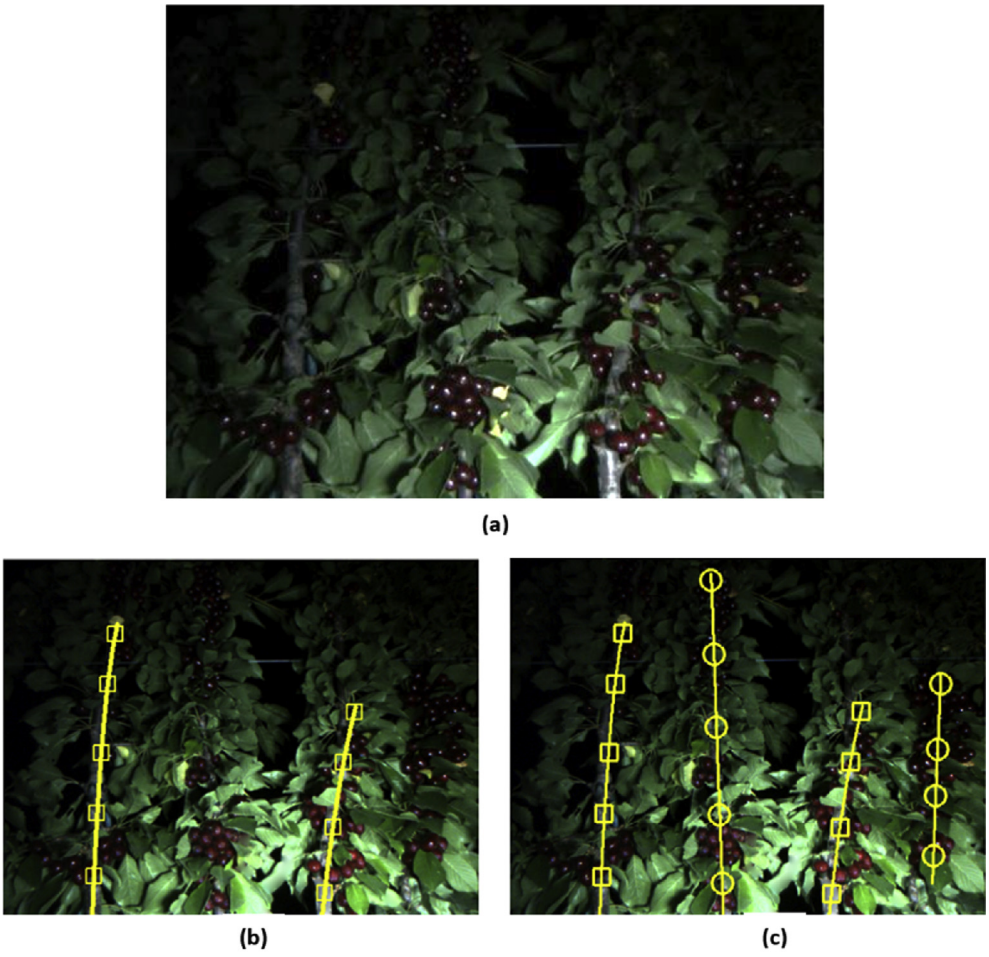

Fig. 8 – An example result of the branch detection method; a) original image of a cherry tree; b) branches identified using only the branch pixels, and c) branches identified using branch and cherry pixels combined; square markers represent branches identified using branch pixels, and circular markers represent branches identified using cherry pixels.

Table 3 – Results of branch detection method based on branch pixels and cherry pixels.

	Based on branch pixels		Based on cherry pixels		Overall		Unidentified	Total
	Detected	False positives	Detected	False positives	Detected	False positives		
Number of branches	249	21	176	35	425	56	28	453
Percentage (%)	55.0	4.6	38.8	7.7	93.8	12.4	6.2	

It was observed that the main source of false positive branch detections came from specular reflections from leaves and low spacing between branches in some poorly trained trees leading to falsely segmented branch regions. Improvement in image classification method to decrease false positive pixels during segmentation may help reduce false detection of branches. In addition, a well-trained orchard with consistent spacing between branches could be

helpful in reducing false positives. About 6.2% of branches were still unidentified after integrated branch detection method. False negative cases were primarily caused by poor lighting on the upper part of the tree canopy as well as thin branches with low fruit density.

The branch detection algorithm was implemented in MATLAB on a computer (Intel(R) Core(TM) i7-2600 CPU @ 3.40 GHz, 8 GB RAM, 64-bit operating system), which took approximately 30 s to process each image having 3–4 branches on average.

Improving the illumination condition during image acquisition without inducing specular reflections could be helpful in reducing unidentified branches and improving overall performance of the branch detection method.

4. Conclusion

Automated sweet cherry harvesting can be achieved with the aid of machine vision system for locating tree branches and guiding harvesting actuators to the desired locations for shaking. The main challenge for machine vision system is detecting branches in tree canopies with full foliage when a lot of branches are occluded. In this study, a branch detection algorithm was developed to identify cherry tree branches in canopies with full foliage during the harvest season. The study was conducted in a cherry orchard trained in Y-trellis architecture. Bayesian classification method was used to classify image pixels into branches, cherries, leaves and background achieving classification accuracies of 81.4% and 95.5% for branches and cherries respectively. Segmented branch and cherry regions were used for the branch detection. Firstly, sections of partially visible branches were used to reconstruct entire branches based on the geometrical properties of segmented branch regions. Secondly, cherry clusters in the images were used to locate the branches that were totally occluded by the foliage and fruit itself. Based on branch pixels only, 55.0% of cherry branches were identified, whereas the detection accuracy was improved by 38.8% using cherry clusters leading to the overall branch detection accuracy of 93.8%. Integration of branch and cherry pixel regions resulted in improved overall branch detection accuracy.

This study showed potential for branch detection in full foliage, which can lead to an automated cherry harvesting system in the future. Further improvement in the performance of this method might be possible by improving pixel classification technique, uniform illumination in imaging region, and proper training of trees ensuring well-spaced vertical branches. The next step in automating shake-and-catch harvesting of sweet cherries is to locate the shaking positions in the detected cherry tree branches. The position of tree branches has been detected along with the position of cherries in the detected branches. Therefore, based on the location of cherry clusters in the canopy, location of suitable shaking points for removing cherries has to be estimated for guiding mechanical shakers to the desired positions.

Acknowledgements

This work was supported in part by the USDA National Institute of Food and Agriculture (NIFA), Hatch project #1005756 and project #1001246 received from Washington State University Agricultural Research Center. Any opinions, findings, conclusions, or recommendations expressed in this publication are those of the author(s) and do not necessarily reflect the view of the U.S. Department of Agriculture.

REFERENCES

Amatya, S., Karkee, M., Gongal, A., Zhang, Q., & Whiting, M. D. (2016). Detection of cherry tree branches in planar architecture for automated sweet cherry harvesting. *Biosystems Engineering, 146*, 3–15.

Ampatzidis, Y. G., & Whiting, M. D. (2013). Training system affects sweet cherry harvest efficiency. *HortScience, 48*(5), 547–555.

Baeten, J., Donne, K., Boedrij, S., Beckers, W., & Claesen, E. (2008). Autonomous fruit picking machine: a robotic apple harvester. *Field and Service Robotics, 42*, 531–539.

Blanco-Roldán, G. L., Gil-Ribes, J. A., Kouraba, K., & Castro-García, S. (2009). Effects of trunk shaker duration and repetitions on removal efficiency for the harvesting of oil olives. *Applied Engineering in Agriculture, 25*(3), 329–334.

Chen, D., Du, X., Zhang, Q., Whiting, M., Scharf, P., & Wang, S. (2012). Performance evaluation of mechanical cherry harvesters for fresh market grade fruits. *Applied Engineering in Agriculture, 28*(4), 483–489.

Du, X., Chen, D., Zhang, Q., Scharf, P. A., & Whiting, M. D. (2011). *Mechanical harvesting of UFO cherry: Investigation of tree plant dynamics* (ASABE paper no. 1110523). St. Joseph, Mich.: ASABE.

Duda, R. O., Hart, P. E., & Stork, D. G. (1973). *Pattern classification* (2nd ed.). A Wiley-Interscience Publication, ISBN 0-471-05669-3.

Erdoğan, D., Güner, M., Dursun, E., & Gezer, I. (2003). Mechanical harvesting of apricots. *Biosystems Engineering, 85*(1), 19–28.

Gonzalez, R. C., & Woods, R. E. (2002). *Digital image processing* (2nd ed.). Upper Saddle River, NJ: Prentice Hall.

He, L., Zhou, J., Du, X., Chen, D., Zhang, Q., & Karkee, M. (2012). *Shaking energy delivery on sweet cherry trees in different excitation models* (ASABE paper no. 12-1337766). St. Joseph, Mich.: ASABE.

Karkee, M., & Adhikari, B. (2015). Reconstruction of apple trees for automated pruning using three dimensional machine vision system. *The Transactions of the ASABE, 58*(3), 565–573.

Karkee, M., Adhikari, B., Amatya, S., & Zhang, Q. (2014). Identification of pruning branches in tall spindle apple trees for automated pruning. *Computers and Electronics in Agriculture, 103*, 127–135.

Kurtulmus, F., Lee, W. S., & Vardar, A. (2014). Immature peach detection in color images acquired in natural illumination conditions using statistical classifiers and neural network. *Precision Agriculture, 15*(1), 57–79.

Larbi, P. A., & Karkee, M. (2014). Effects of orchard characteristics and operator performance on harvesting rate of a mechanical sweet cherry harvester. *GSTF Journal on Agricultural Engineering, 1*(1), 1–11.

Li, P., Lee, S., & Hsu, H. Y. (2011). Review on fruit harvesting method for potential use of automatic fruit harvesting systems. *Procedia Engineering, 23*, 351–366.

Long, L. E. (2010). *Worldwide trends in cherry training systems*. Available at: http://extension.oregonstate.edu Accessed 06.07.15.

Parameswarakumar, M., & Gupta, C. P. (1991). Design parameters for vibratory mango harvesting system. *Transactions of the ASAE, 34*(1), 14–20.

Peterson, D. L., Bennedsen, B. S., Anger, W. C., & Wolford, S. D. (1999). A system approach to robotic bulk harvesting of apples. *Transactions of ASAE, 42*(4), 871–876.

Peterson, D. L., Whiting, M. D., & Wolford, S. D. (2003). Fresh-market quality tree fruit harvester, part I: sweet cherry. *Applied Engineering in Agriculture, 19*(5), 539–543.

Peterson, D. L., & Wolford, S. D. (2001). Mechanical harvester for fresh market quality stemless sweet cherries. *Transactions of the ASAE, 44*(3), 481–485.

Polat, R., Geber, I., Guner, M., Dursun, E., Erdogan, D., & Bilim, H. C. (2006). Mechanical harvesting of pistachio nuts. *Journal of Food Engineering, 79*(4), 1131–1135.

Seavert, C., Freeborn, J., & Long, L. (2008). *Orchard economics: Establishing and producing high-density sweet cherries in Wasco County*. OSU Extension Service Publication (EM 8802-E).

Shapiro, L. G., & Stockman, G. C. (2001). *Computer vision*. Upper Saddle River, New Jersey: Prentice-Hall, Inc., ISBN 0-13-030796-3

Slaughter, D. C., & Harrell, R. C. (1989). Discriminating fruit for robotic harvest using color in natural outdoor scenes. *Transactions of the ASAE, 32*(2), 757–763.

Tabb, A. (2009). *Three-dimensional reconstruction of fruit trees by a shape from silhouette method* (ASABE paper no. 096138). St. Joseph, Mich.: ASABE.

Tanigaki, K., Fujiura, T., Akase, A., & Imagawa, J. (2008). Cherry harvesting robot. *Computers and Electronics in Agriculture, 63*, 65–72.

Wang, Q., & Zhang, Q. (2013). *Three-dimensional reconstruction of a dormant tree using RGB-D cameras* (ASABE paper no. 131593521). St. Joseph, Mich.: ASABE.

Whiting, M. D. (2009). *Upright fruiting offshoots*. Prosser, WA: WSU-IAREC. Available at: http://cahnrs-cms.wsu.edu/StoneFruit/research/Pages/ufo.aspx Accessed 06.05.15.